Journal of Solution Chemistry (2019) 48:1535–1546
https://doi.org/10.1007/s10953-019-00932-9

An Experimental Study to Synthesize and Characterize Host–Guest Encapsulation of Anthracene, and the Quenching Effects of Co and Ni

Sinem Ezgi Sarlı[1] · **Umit Ay**[1]

Received: 1 April 2019 / Accepted: 8 August 2019 / Published online: 18 November 2019

Abstract
A complex of anthracene with methyl-beta-cyclodextrin (A-Me-β-CD) having fluorophoric characteristics was obtained in aqueous medium. Spectroscopic and thermal analyses of the complex were performed by Fourier transform infrared spectroscopy and differential scanning calorimetry-thermogravimetry. The interaction of Me-β-CD and anthracene was also analyzed by means of spectrometry by a UV–Vis spectrophotometer. The stoichiometry of the complex was determined by the Benesi–Hildebrand method. The complex formation constant was found to be $(42 \pm 3) \times 10^3$ L·mol^{-1}. The Gibbs energy and excited singlet state energy were calculated. The mechanism of the quenching effect of Co(II) and Ni(II) metals in the inclusion complex was studied. The Stern–Volmer constant, bimolecular quenching rate constant, lifetime and approximate activation energy values were determined, and the quenching was found to be diffusion controlled dynamic quenching. In addition, with the energy band calculations made, it was shown by means of Taug curves that electron transfer was made to Ni and Co metals from the complex fluorophore group in the quenching mechanism.

Keywords Anthracene · Encapsulation · Lifetime · Band gap · Fluorescence

1 Introduction

Cyclodextrins (CDs) are bucket-shaped oligosaccharide compounds with hydrophilic and hydrophobic groups. There are three types: alpha (α-CD), beta (β-CD) and gamma (γ-CD) cyclodextrin in nature. Among these α-cyclodextrin is not suitable for many drugs and γ-cyclodextrin is expensive. The most commonly used and best known are β-CDs [1–3].

Electronic supplementary material The online version of this article (https://doi.org/10.1007/s10953-019-00932-9) contains supplementary material, which is available to authorized users.

✉ Umit Ay
umurege@kocaeli.edu.tr; umitay36@hotmail.com

Sinem Ezgi Sarlı
sinamezgisarli@gmail.com

[1] Department of Chemistry, Kocaeli University, 41380 Kocaeli, Turkey

β-CD is widely used because it is readily available, and its cavity size is suitable for a wide range of guest molecules [4]. The internal cavity is about 0.8 nm deep and 0.7 nm in diameter, providing a hydrophobic chiral environment for small organic guest molecules. β-CDs are highly prone to inclusion complex formation. High energy water molecules are exposed during complex formation [5, 6]. They dissolve very little in water. That is why their use in the pharmaceutical industry is very limited. However, their solubility in water has been increased by modification [7]. There are many studies on the use of anthracene as a probe molecule in the literature. However, there are few studies describing the effect of heavy metals on the inclusion complex. There are even fewer studies on the quenching mechanism.

This study, unlike the previous study on anthracene-Me-β-CD [8], attempts to elucidate the quenching mechanism. In this study, two different transition metals, Co and Ni, were selected and the inclusion complex formed by anthracene was re-synthesized at 25 ± 1 °C. It was a very interesting study to see the effect of changing the working conditions on the results. When compared with the previous study, it was seen that the change in ambient temperature, mixing speed and residence time in water bath affected the complex formation constant and quantum yield. With energy band calculations and fluorescence lifetime measurements, the quenching mechanism of Co(II) and Ni(II) metals were revealed.

2 Experimental

2.1 Chemicals and Instruments

Me-β-CD (mean molecular weight = 1310 g·mol^{-1}), anthracene (99%) and ludox-AS-30 colloidal silica (standard form used for lifetime measurements) were obtained from Sigma-Aldrich Chemie Gmbh and ethanol from Merck, Darmstadt. All solutions of metal ions were prepared from analytical grade nitrate salts (Merck, Darmstadt) dissolved in doubly distilled water. All other chemicals were of analytical-reagent grade and were used as received without further purification. A Varian Agilent Cary Eclipse instrument was used for fluorescence measurements.

2.2 Formation of Inclusion Complex

The concentration of Me-β-CD was kept constant at 10^{-3} mol·L^{-1}, while the concentration of anthracene varies between 10^{-3} and 10^{-5} mol·L^{-1}. The top of the beaker on the hot plate was closed with a watch glass. The solutions were stirred at room temperature for 24 h by magnetic stirrer. The solutions were kept in an ultrasonic bath for about 2 min before being transferred to the volumetric flasks. Finally, they were transferred to 100 mL volumetric flasks and complexes were formed at 25 ± 1 °C. The effect of mixing time on inclusion complex formation was clearly seen in our previous studies with anthracene [8]; mixing times of less than 24 h affect the quantum yield and the complex formation constant. No effects were observed after more than 24 h. Therefore, in this study, 24 h were selected for inclusion complex formation with anthracene. The inclusion complexes obtained were characterized by different physical and spectroscopic methods. In all calculations, complex formation constant and quantum yield values obtained by re-synthesis of the complex were used. As mentioned hereinabove, the change in experimental conditions influenced these two values. Heavy metals were added directly into 1.5 mL of complex solutions by

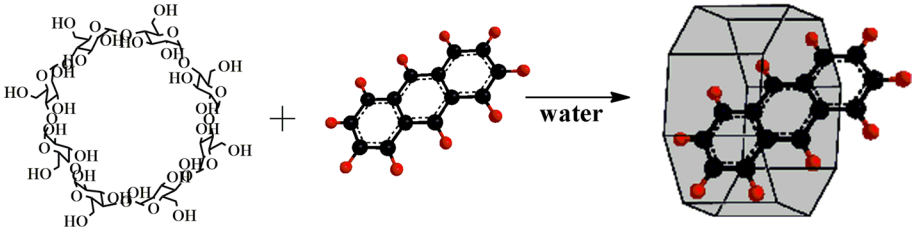

Scheme 1 Formation of inclusion complex

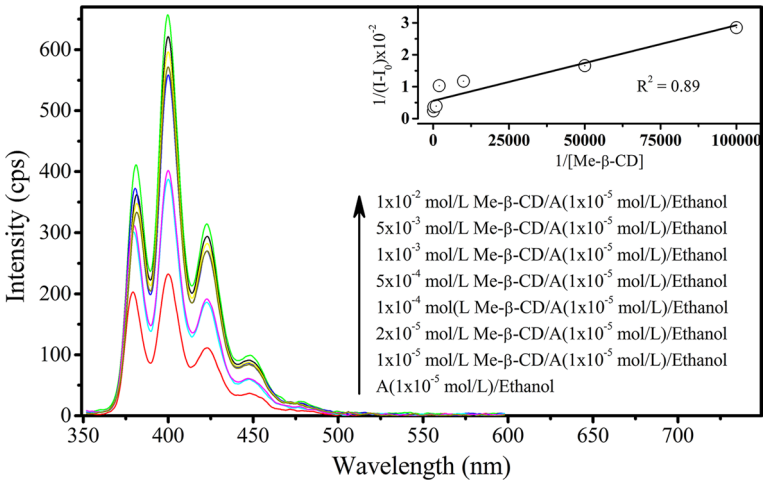

Fig. 1 The effect of increasing methyl-β-cyclodextrin concentration on the fluorescence spectrum of the anthracene dissolved in 1×10^{-5} mol·L^{-1} ethanol. Benesi–Hildebrand graph ($1/[I-I_0]$ vs 1/[Me-β-CD]) (graphic inside) ($\lambda_{ex}=360$ nm)

means of a micro-pipette. Changes in fluorescence intensity were observed at 25 ± 1 °C. The emission spectra were recorded at an excitation wavelength of 360 nm.

The synthesized complex is shown in Scheme 1.

3 Results and Discussion

Since Co and Ni metals do not have fluorescence, the quenching effect of these two metals was investigated using anthracene. A probe molecule was successfully prepared. The photo physical properties of the excited level of heavy metals and inclusion complexes were monitored. The stoichiometry of the complex was found to be 1:1 with the Benesi–Hildebrand method [9]. The binding constant, K_b, was found to be $(42\pm3)\times10^3$ L·mol^{-1} from the slope of the graph (Fig. 1). The magnitude of this value indicates the formation of a strong inclusion complex. In addition, the stability of the complex was tested for 4 weeks. At the end of this period, the intensity of the emission decreased by 22%. This shows that the complex formed is stable over a long period of time (Fig. 2). Figures 3 and 4 show how Co(II) and Ni(II) metals change the

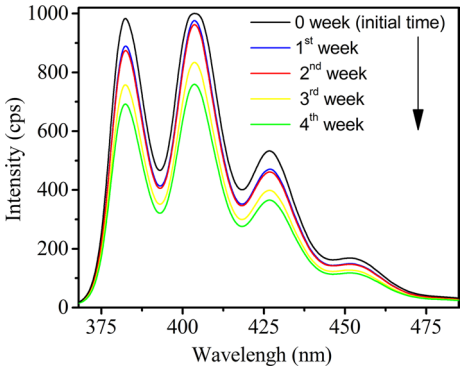

Fig. 2 The stability of inclusion complex

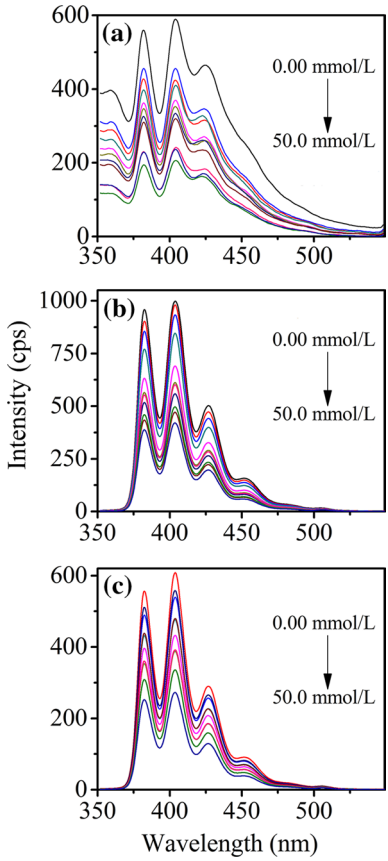

Fig. 3 **a** Quenching effect of cobalt on 10^{-3} mol·L^{-1} anthracene. **b** Quenching effect of cobalt on 10^{-4} mol·L^{-1} anthracene. **c** Quenching effect of cobalt on 10^{-5} mol·L^{-1} anthracene, [Co^{2+}] = 0.1 mol·L^{-1}. (λ_{ex} = 360 nm)

fluorescence intensity. All results relating to these two metals are given in Table 1. In Fig. 5, the K_{S-V} value was calculated from the Stern–Volmer plot (I_0/I versus [Q]). The linearity of this graph suggests that the quenching is dynamic. After lifetime

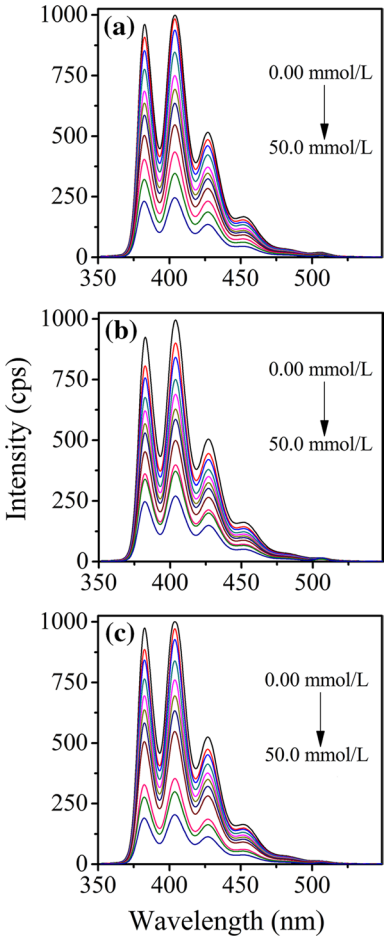

Fig. 4 **a** Quenching effect of nickel on 10^{-3} mol·L^{-1} anthracene. **b** Quenching effect of nickel on 10^{-4} mol·L^{-1} anthracene. **c** Quenching effect of nickel on 10^{-5} mol·L^{-1} anthracene, $[Ni^{2+}] = 0.1$ mol·L^{-1}. ($\lambda_{ex} = 360$ nm)

Table 1 Stern–Volmer (K_{S-V}) constants, R^2 values and quantum yields in the presence and absence of quenching reagent

Heavy metal	Electronic configuration	Concentration (mol·L^{-1})	K_{S-V} (L·mol^{-1})	R^2	$\phi_{FQ} - \phi_F$
Co	$4s^2 3d^7$	10^{-3}	31 ± 2	0.98	
		10^{-4}	26 ± 2	0.93	0.07–0.24
		10^{-5}	17 ± 1	0.94	
Ni	$4s^2 3d^8$	10^{-3}	55 ± 5	0.93	
		10^{-4}	47 ± 4	0.95	0.06–0.34
		10^{-5}	72 ± 7	0.92	

[Me-β-CD] = 1×10^{-3} mol·L^{-1}

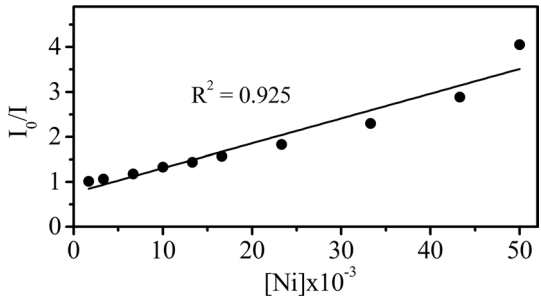

Fig. 5 Stern–Volmer graph for Ni^{2+}

measurements, it will be possible to give a clearer answer on the exact nature of the quenching mechanism.

For quantum yield calculations, 9,10 diphenyl anthracene was used as the reference material [10, 11]. The complexes formed by many transition metal ions contain incomplete d orbitals. This quenches the fluorescence in the solution medium.

Many coordinated transition metal ions are paramagnetic. For such a system, the following equation may be written (1);

$$S_1^*(\text{Ni–Me} - \beta - \text{CD/A.}) - \text{I.S.C} \rightarrow T_1(\text{Ni–Me} - \beta - \text{CD/A.}) - Q \rightarrow S_0(\text{Ni–Me} - \beta - \text{CD/A.}) \quad (1)$$

where S_1^* the excitation may be the transition from the first singlet state (S_1^*) to the triplet state (T_1) and then back to the singlet state (S_0). The quantum yield (ϕ_F) of anthracene–Me-β-CD (A–Me-β-CD) was calculated to be 0.3444 in the absence of heavy metal ions (Co and Ni). The amount of added cobalt and nickel salts varied, i.e., varying the amount of quencher, giving quantum yields from 0.3444 to 0.0591. The quenching of the A–Me-β-CD inclusion complex results in an electron donation from the fluorophore group to the quencher. This suggests that electron transfer is highly compatible with the results of the energy band values given below.

The energy band of A–Me-β-CD, A–Me-β-CD–Co and A–Me-β-CD–Ni can be calculated by using the following equations

$$E_{VB} = X - E^e + 0.5E_g \quad (2)$$

$$E_{CB} = E_{VB} - E_g \quad (3)$$

where E_{VB} and E_{CB} are the band edge potentials of the valence and the conduction bands, respectively. X is the geometric mean of the absolute electro-negativity of the constituent atoms on the Pearson scale (PAE), E_g is the band gap and E^e is the energy of the electrons on the hydrogen scale is usually taken ~4.5 eV [12].

The PAE values of constituent atoms and band structure parameters of the A–Me-β-CD (inclusion complex), inclusion complex–Co and inclusion complex–Ni calculated by using the Eqs. 2 and 3 are listed in Table 2, where filling affects the value of E_{CB} to a certain degree.

While the E_{CB} value for inclusion complex was calculated as 0.073 eV, it is 0.44 eV in the presence of nickel as quencher. Furthermore, this result is fits in nicely with the results by Kumar et al. [13] where they have reported that there can be an electron transfer from components with lower E_{CB} values to those with higher E_{CB} values. The calculated E_{CB} value for the inclusion complex is 0.073 eV, which is much lower than that of nickel

Table 2 PAE values of constituent atoms and band structure parameters

	C	H	O	N	Fe	Mn
PAE (eV)	6.27	7.18	7.54	7.30	4.06	3.72
		E_{CB} (eV)	E_{VB} (eV)		X (eV)	E_g (eV)
Samples						
A–Me-β-CD		0.07	4.91		6.99	4.834
A–Me-β-CD–Co		0.43	4.53		6.98	4.091
A–Me-β-CD–Ni		0.44	4.52		6.98	4.086

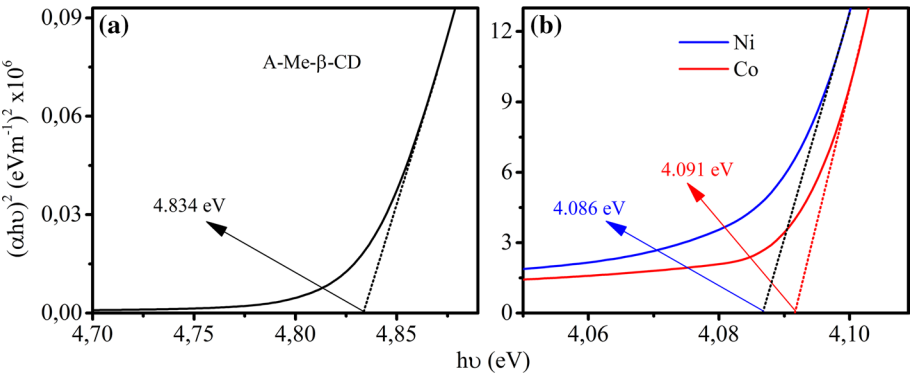

Fig. 6 Tauc's plots of **a** inclusion complex and **b** metal quenchers

(0.44 eV) and cobalt (0.43 eV). This indicates that there may be an electron transfer from the inclusion complex to nickel and cobalt (Fig. 6).

The heavy metals with the stronger quenching effect depend on its electronegativity or paramagnetism/diamagnetism. Nickel may be a more effective quencher due to its high electronegativity compared to cobalt.

3.1 Lifetime

The fluorescence lifetimes were obtained using a Horiba–Jobin–Yvon–SPEX Fluorolog 3-2iHR instrument with a Fluoro Hub-B Single Photon Counting Controller at an excitation wavelength of 470 nm. Signal acquisition was performed using a TCSPC module (NanoLED-390 emitting 390 nm). The lifetime values of the inclusion complexes were first read in the absence of the quencher and the presence of the quencher (Fig. 7).

Using the fluorescence lifetime value measured in the absence of the quencher, the bimolecular quenching rate constants for Co^{2+} and Ni^{2+} i.e., k_q values, have been calculated to be $(6.6 \pm 0.3) \times 10^9$ L·mol^{-1}·s^{-1} and $(12 \pm 1) \times 10^9$ L·mol^{-1}·s^{-1}, respectively [14]. These values are not greater than the diffusion rate constant. The mechanism of the quenching phenomenon is dependent on molecular dynamic diffusion. The calculated bimolecular quenching rate constant values (k_q) should be approximately equal to 6.6×10^9 L·mol^{-1}·s^{-1} when the observed phenomenon is diffusion controlled. Here, it is seen that these values

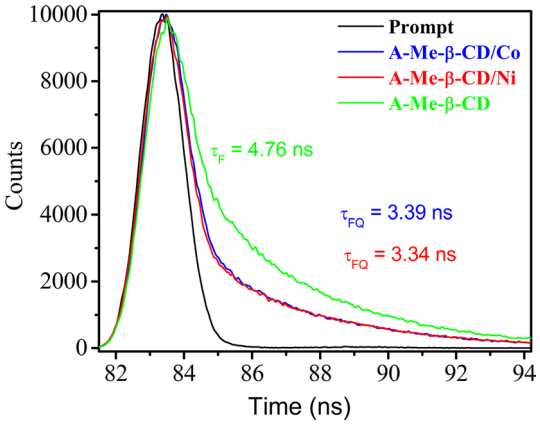

Fig. 7 Fluorescence lifetime graph of the A–Me-β-CD inclusion complex in the presence and absence of the quencher reagent (in the presence of Co(II) and Ni(II) as quenchers)

are approximately equal for both metals, too. The approximate quenching activation energy values were was 6.7 kJ·mol^{-1} for cobalt and 5.3 kJ·mol^{-1} for nickel [15].

3.2 Characterization of Inclusion Complexes

3.2.1 FT-IR Spectral Analysis

A Bruker-Alpha model device was used for FT-IR measurements. The FT-IR technique is one of the most important and powerful techniques to confirm inclusion complex formation between anthracene (A) and Me-β-CD. Stanculescu et al. [16] studied the interaction of β-CD with polychlorophenol compounds in aqueous media using FT-IR and molecular modeling techniques. This study, too, displays the interaction of Me-β-CD with anthracene by employing the FT-IR technique. The FT-IR spectra of 10^{-3} mol·L^{-1} Me-β-CD and 10^{-3} mol·L^{-1} A–Me-β-CD inclusion complex are shown in Fig. 8. In the aqueous solution, the strong O–H tensile band at 3300 cm^{-1} of water has been reported in the literature to reduce the spectral contrast of the aromatic C–H stretching bands between 3150 and 2900 cm^{-1} [17]. In this study, despite the influence of the O–H band,

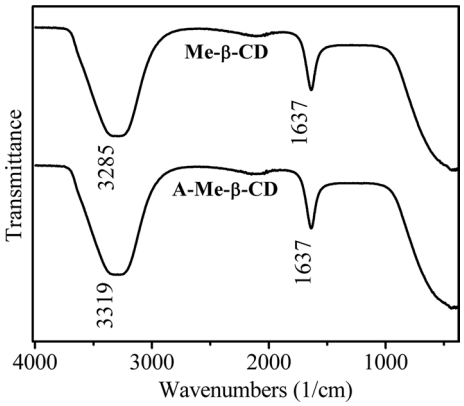

Fig. 8 FT-IR spectra of Me-β-CD and A–Me-β-CD

a significant shift of about 34 cm^{-1} in the C–H stretching vibration confirms the formation of an inclusion complex.

3.2.2 UV–Vis Spectroscopy

A PG Instrument T70+ model spectrophotometer was used for measurement of absorption spectra. The complex formation leads to a change in the absorption spectrum of the guest molecule [18–20]. During the spectral changes, the chromophore of the guest is transferred from an aqueous medium to the non-polar cyclodextrin. These changes must be due to a perturbation of the electronic energy levels of the guest caused either by direct interaction with the cyclodextrin, by the exclusion of solvating water molecules or by a combination of these two effects [21, 22]. Small shifts are observed in the UV spectra of the included guests, the method is often used to detect inclusion complexation [23–26]. Hypsochromic or bathochromic shifts or increases in the absorptivity without change in the λ_{max} have been considered as evidence for interaction between cyclodextrin and anthracene in the formation of the complex. Figure 9 shows the absorption spectrum of anthracene and inclusion complex. As described above, even the slightest shift in the UV spectrum indicates inclusion complex formation.

3.2.3 Thermal Analysis

Thermal analyses were performed by differential scanning calorimetry (DSC, Perkin Elmer DSC 4000) and thermogravimetry (TG, Perkin Elmer TGA 4000) between 25–350 and 40–900 °C, respectively with a 10 °C·min^{-1} heating rate (atmosphere N_2; flow 20 mL·min^{-1}). Figure 10 shows DSC thermograms of the samples. The endothermic peak seen in the DSC thermogram of anthracene at about 215 °C is the characteristic melting peak of anthracene, as indicated by Li et al. [27]. The most striking feature of the DSC thermograms was that the melting peak observed at around 215 °C for anthracene was not observed in the thermogram of the inclusion complex A–Me-β-CD. The disappearance of this melting peak associated with the crystalline fraction may be largely due to the amorphous structure of the inclusion complex. It is evident in both the DSC curve and the TG curve that the complex begins to degrade at 300 °C and with a loss of mass.

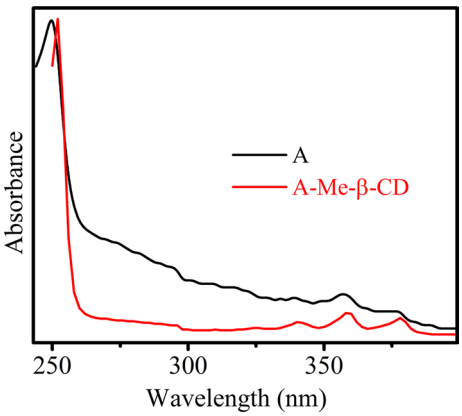

Fig. 9 Absorption spectrum of anthracene and A–Me-β-CD in 10^{-3} mol·L^{-1} aqueous solution

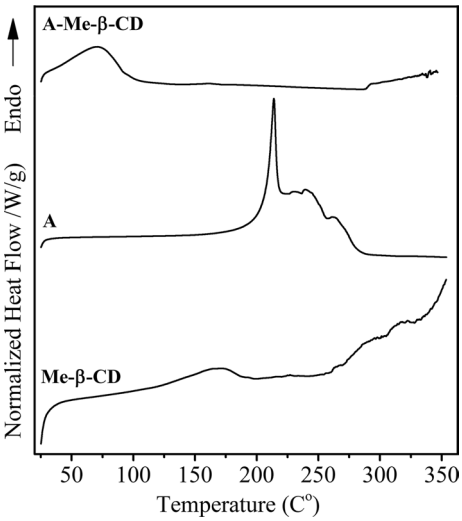

Fig. 10 DSC thermogram Me-β-CD, anthracene (A) and inclusion complex (DSC, temperature accuracy: ± 0.1 °C)

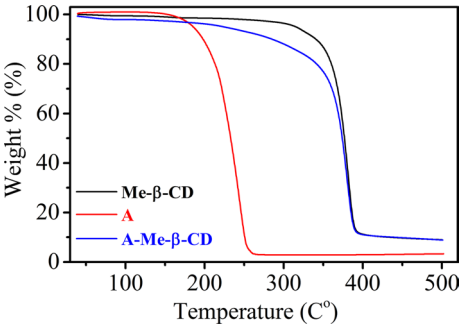

Fig. 11 TGA degradation curves of the samples (temperature accuracy: ± 1 °C and balance accuracy: ± 0.02%)

As seen from TG curves (Fig. 11), the thermal stability of the complex is lower than that of Me-β-CD. This may be due to the presence of Me-β-CD instead of an inclusion complex. Furthermore, as can be seen from the Supplementary Material, the initial onset temperature for degradation of the complex was substantially increased by about 150 °C. This promotes complex formation with anthracene and Me-β-CD.

4 Conclusion

Our previous study investigated whether lead or cadmium metals had greater quenching on the inclusion complex formed by the anthracene. Based on the electronegativity difference between the two metals, quenching was increased. Electronegativity values for nickel and cobalt metals are 1.99 and 1.88, respectively. As can be seen, these values are very close to each other. Hence, the inclusion complex was re-synthesized in order to show that not only the electronegativity of these two metals was effective in the quenching but another mechanism could as well be effective. Thermal and spectroscopic characterization of the complex was performed with DSC-TA, FT-IR and UV–Visible spectroscopy. Thanks to the probe molecule, the quenching effect of Co(II) and Ni(II) was investigated. Stern–Volmer and

bimolecular quenching rate constants were calculated. Also, lifetime values were measured in the presence and absence of quenching reagent. As a result of all these measurements and calculations, it was concluded that the quenching event here is diffusion controlled dynamic quenching. At the same time it was shown through Tauc's plots that electrons transfer from the fluorophore group in the inclusion complex to the metal.

Acknowledgements We would like to thank the Kocaeli University Scientific Research Coordinator (BAP) (Project No: 2017/010), who contributed to the authors in this study, and the Gebze Technical University, Department of Chemistry, who helped to read the fluorescence lifetimes.

References

1. Anitha, A., Murugan, M., Rajamohan, R.: Molecular encapsulation of amodiaquine in 2-hydroxypropyl β-cyclodextrin cavity. Characterization and its in vitro cytotoxicity. Spectrosc. Lett. **51**, 198–204 (2018)
2. Murugan, M., Anitha, A., Sivakumar, K., Rajamohan, R.: Supramolecular ınteraction of primaquine with native β-cyclodextrin. J. Solution Chem. **47**, 906–929 (2018)
3. Sabari, C.L., Sivakumar, K., Rajamohan, R.: Improvement of cytotoxic activity of local anesthetics against human breast cancer cell line through the cyclodextrin complexes. J. Macromol. Sci. A **54**, 402–410 (2017)
4. Sambasevam, K.P., Mohamad, S., Sarih, N.M., Ismail, N.A.: Synthesis and characterization of the ınclusion complex of β-cyclodextrin and azomethine. Int. J. Mol. Sci. **14**, 3671–3682 (2013)
5. Norkus, E.: Metal ion complexes with native cyclodextrins. An overview. J. Incl. Phenom. Macrocycl. Chem. **65**, 237–248 (2009)
6. Kemtong, C., Banerjee, D., Liu, Y., El Khoury, J.M., Rinaldi, P.L., Hu, J.: Formation of an ınclusion complex of a new transition metal ligand in β-cyclodextrin. Supramol. Chem. **17**, 335–341 (2005)
7. Jullian, C., Brossard, V., Gonzalez, I., Alfaro, M., Olea-Azar, C.: Cyclodextrins-kaempferol ınclusion complexes: spectroscopic and reactivity studies. J. Solution Chem. **40**, 727–739 (2011)
8. Ay, U., Dogruyol, Z., Arsu, N.: The effect of heavy metals on the anthracene-me-β-cyclodextrin host-guest ınclusion complexes. Supramol. Chem. **26**, 66–70 (2014)
9. Ay, U., Sarlı, S.E.: Investigation by fluorescence technique of the quenching effect of Co^{2+} and Mn^{2+} transition metals, on naphthalene-methyl-beta-cyclodextrin host-guest ınclusion complex. J. Fluoresc. **28**, 1371–1378 (2018)
10. Morris, J.V., Mahoney, M.A., Huber, J.R.: Fluorescence quantum yield determinations. 9,10-dipenylanthracene as a reference standard in different solvents. J. Phys. Chem. **80**, 969–974 (1976)
11. Balta, D.K., Temel, G., Aydın, M., Arsu, N.: Thioxanthone based water-soluble photoinitiators for acrylamide photopolymerization. Eur. Polym. J. **46**, 1374–1379 (2010)
12. Ozkazanc, E., Ozkazanc, H., Gundogdu, O.: Characterization and charge transport mechanism of multifunctional polyfuran/tin(IV) oxide composite. J. Inorg. Organomet. **28**, 2108–2120 (2018)
13. Kumar, A., Kumar, A., Sharma, G., Al-Muhtaseb, A.H., Naushad, M., Ghfar, A.A., Stadler, F.J.: Quaternary magnetic BiOCl/g-C3N4/Cu2O/Fe3O4 nano-junction for visible light and solar powered degradation of sulfamethoxazole from aqueous environment. Chem. Eng. J. **334**, 462–478 (2018)
14. University of Zurich, Department of Chemistry Home Page. https://www.chem.uzh.ch/de/study/download/year2/che211.html
15. Baggott, J.E., Pilling, M.J.: Temperature dependence of excited-state electron-transfer reactions quenching of RuL32+ emission by copper(II) and europium(III) in aqueous solution. J. Phys. Chem. **84**, 3012–3019 (1980)
16. Stanculescu, I., Dobrica, I., Mandravel, C., Mindrila, G.: Anal. Univ. Bucuresti-Chimie (serienoua) **19**, 47 (2010)
17. Drössler, P., Holzer, W., Penzkofer, A., Hegemann, P.: Fluoresence quenching of riboflavin in aqueous solution by methionin and cystein. Chem. Phys. **286**, 409–420 (2003)
18. Marzouqi, A.H.A., Shehatta, I., Jobe, B., Dowaidar, A.: Phase solubility and inclusion complex of Itraconazole with ß-cyclodextrin using supercritical carbon dioxide. J. Pharm. Sci. **95**, 292–304 (2006)
19. Jadhav, G.S., Vavia, P.R.: Physicochemical, in silico and in vivo evaluation of a Danazol–β-cyclodextrin complex. Int. J. Pharm. **352**, 5–16 (2008)

20. Chow, D.D., Karara, A.K.: Characterization, dissolution and bioavailabilty in rats of Ibuprofen-β-cyclodextrin complex system. Int. J. Pharm. **28**, 95–101 (1986)
21. Uekama, K., Fujinaga, T., Otagiri, M., Hirayama, F., Yamasaki, M.: Inclusion complexations of steroid hormones with cyclodextrins in water and in solid phase. Int. J. Pharm. **10**, 1–15 (1982)
22. Rajagopalan, N., Chen, S.C., Chow, W.S.: A study of the inclusion complex of Amphotericin-B with γ-cyclodextrin. Int. J. Pharm. **29**, 161–168 (1986)
23. Uekama, K., Narisawa, S., Hirayama, F., Otagiri, A.: Improvement of dissolution and absorption characteristics of benzodiazepines by cyclodextrin complexation. Int. J. Pharm. **16**, 327–338 (1983)
24. Smulevich, G., Feis, A., Mazzi, G., Vincieri, F.F.: Inclusion complex formation of 1,8-dihydroxyanthraquinone with cyclodextrins in aqueous solution and in solid state. J. Pharm. Sci. **77**, 523–526 (1988)
25. Xiang, T.X., Andersoon, B.D.: Inclusion complexes of purine nucleosides with cyclodextrins: II. Investigation of inclusion complex geometry and cavity microenvironment. Int. J. Pharm. **59**, 45–55 (1990)
26. Singh, R., Bharti, N., Madan, J., Hiremath, S.N.: Characterization of cyclodextrin ınclusion complexes: a review. J. Pharm. Sci. Technol. **2**, 171–183 (2010)
27. Ye, C.P., Ding, X.X., Li, W.Y., Mu, H., Wang, W., Feng, J.: Determination of crystalline thermodynamics and behavior of anthracene in different solvents. AIChE J. **64**, 2160–2167 (2018)